Supplementary Information

Figure S1 Low-energy CID spectra of the complexes (a) **[Cu^{II}(dien)GAW]$^{\bullet 2+}$** and (c) **[Cu^{II}(dien)GGW]$^{\bullet 2+}$** and the species (b) **[GAW]$^{\bullet +}$** and (d) **[GGW]$^{\bullet +}$**.

Figure S2 Comparison of the theoretical IR spectra (black curve) and the experimental IRMPD spectra of the structures of (a) the **[Cu^{II}(dien)GAW]$^{\bullet 2+}$-SB1** complex (magenta), (b) **[GAW$_\pi$$^\bullet$]$^+$-1** (green), and (c) **[Cu^{I}(dien)]$^+$-1** (purple). Theoretical IR spectra were evaluated at the B3LYP/6-311++G(d,p) level. An anharmonicity scaling factor of 0.976 was applied.

Figure S3 Theoretical IR spectra of some selected low-lying geometries of **[Cu^{II}(dien)GGW]$^{\bullet 2+}$**: (a) **SB1**, (b) **SB2**, (c) **SB3**, (d) **SB4**, and (e) **CS** (black curve), with corresponding IRMPD spectra (pink shaded regions). Energies and spin densities were evaluated at the B3LYP/6-311++G(d,p) level. An anharmonicity scaling factor of 0.976 was applied. Relative energies are in kcal mol^{-1}; bond lengths in Å.

Figure S4 Theoretical IR spectra of [indole]$^+$ (blue curve), [indole]$^{\bullet +}$ (black curve), and [indole – H]$^\bullet$ (red curve); wavenumbers: 1500–1600 cm^{-1}.

Figure S5 Theoretical IR spectra of some selected low-lying geometries of (a) **[G$_\alpha$$^\bullet$GW]$^+$**, (b) **[GGW$_\pi$]$^{\bullet +}$**, and (c) **[GGW$_\beta$$^\bullet$]$^+$** (black traces), with relative IRMPD spectra (blue areas). Energies and spin densities were evaluated at the B3LYP/6-311++G(d,p) level. An anharmonicity scaling factor of 0.976 was applied. Relative energies are in kcal mol^{-1}; bond lengths in Å.

Figure S6 PES of hydrogen atom migrations in **[Cu^{II}(dien)GGW]$^{\bullet 2+}$**. Energies and spin densities were evaluated at the B3LYP/6-311++G(d,p) level. The upper numbers are enthalpies at 0 K; the lower numbers in parentheses are free energies at 298 K. Relative energies are in kcal mol^{-1}. Relative energies are presented in kJ mol^{-1} below the PES.

Figure S1

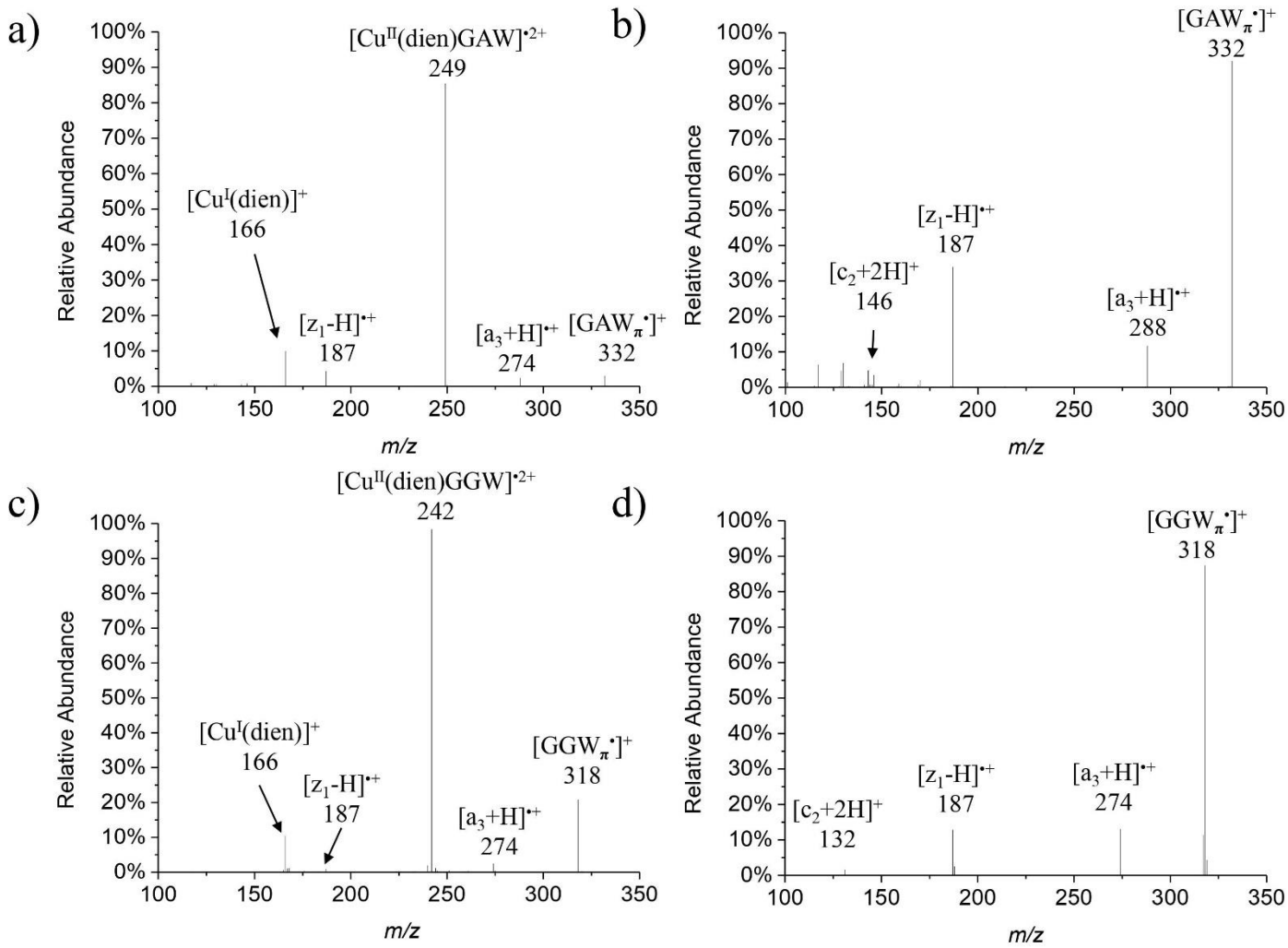
a)
b)
c)
d)
Relative Abundance
m/z
100%
90%
80%
70%
60%
50%
40%
30%
20%
10%
0%
100
150
200
250
300
350
[Cu^II(dien)GAW]•2+
249
[Cu^I(dien)]+
166
[z1-H]•+
187
[a3+H]•+
274
[GAWπ•]+
332
[c2+2H]+
146
[a3+H]•+
288
[Cu^II(dien)GGW]•2+
242
[Cu^I(dien)]+
166
[z1-H]•+
187
[a3+H]•+
274
[GGWπ•]+
318
[c2+2H]+
132
[z1-H]•+
187
[a3+H]•+
274
[GGWπ•]+
318

Figure S2

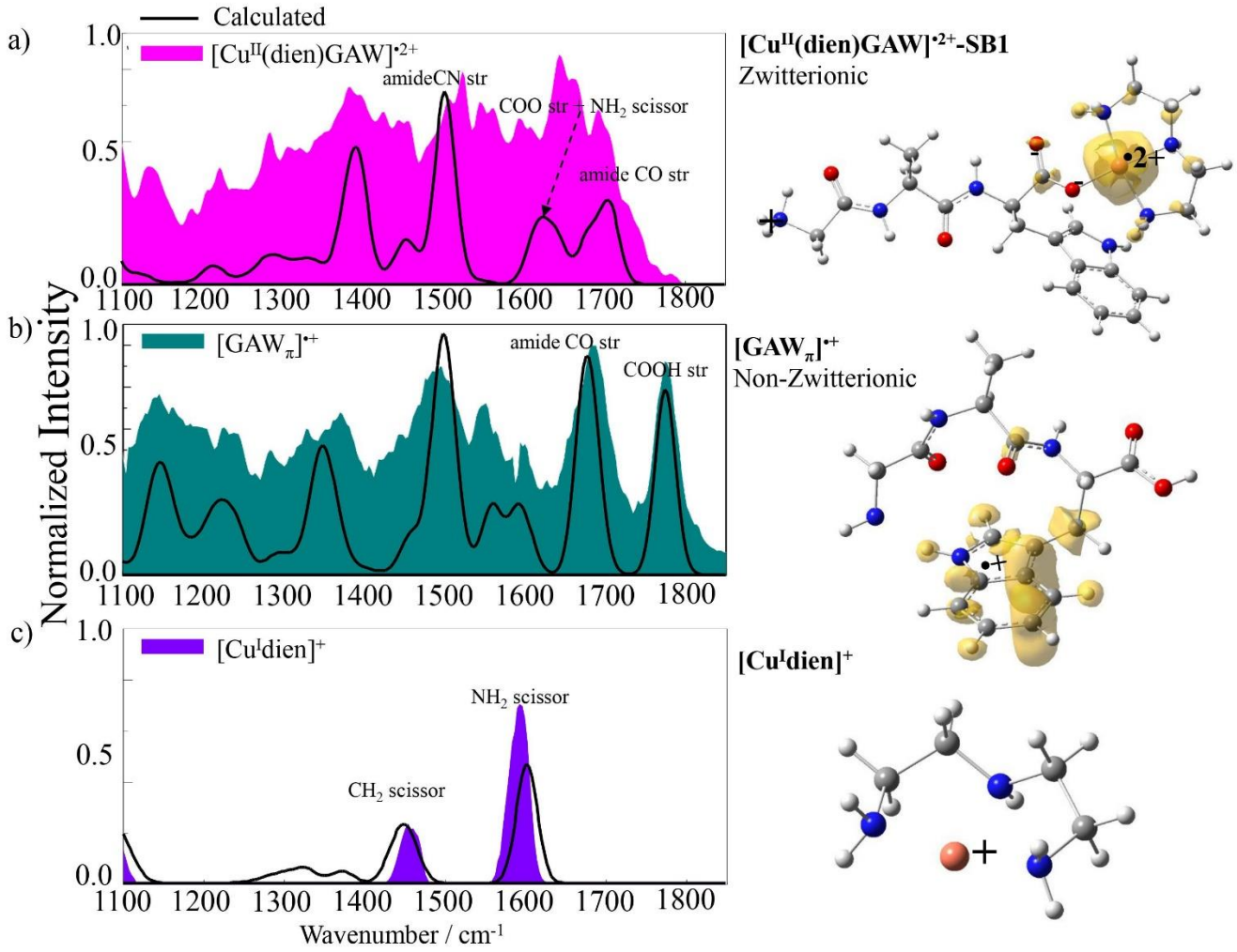
a)
b)
c)
Calculated
[Cu^{II}(dien)GAW]$^{\bullet 2+}$
amideCN str
COO str + NH$_2$ scissor
amide CO str
[GAW$_\pi$]$^{\bullet +}$
amide CO str
COOH str
[Cu^{I}dien]$^{+}$
NH$_2$ scissor
CH$_2$ scissor
Normalized Intensity
Wavenumber / cm^{-1}
[Cu^{II}(dien)GAW]$^{\bullet 2+}$-SB1
Zwitterionic
[GAW$_\pi$]$^{\bullet +}$
Non-Zwitterionic
[Cu^{I}dien]$^{+}$

Figure S3

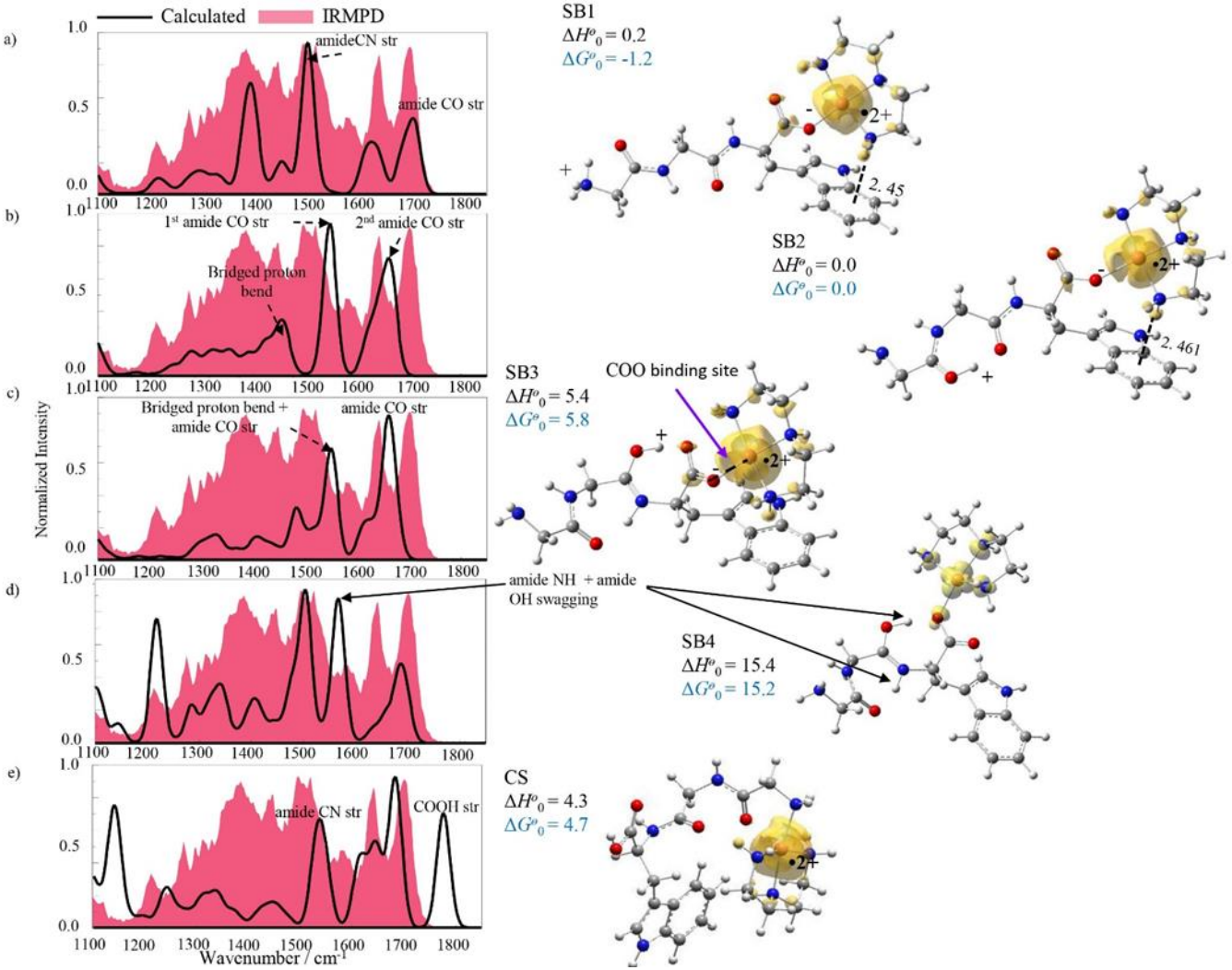
Calculated
IRMPD
a)
amideCN str
amide CO str
b)
1st amide CO str
2nd amide CO str
Bridged proton bend
c)
Bridged proton bend + amide CO str
amide CO str
d)
e)
amide CN str
COOH str
Normalized Intensity
Wavenumber / cm-1
SB1
ΔH°0 = 0.2
ΔG°0 = -1.2
2. 45
SB2
ΔH°0 = 0.0
ΔG°0 = 0.0
2. 461
SB3
ΔH°0 = 5.4
ΔG°0 = 5.8
COO binding site
amide NH + amide OH swagging
SB4
ΔH°0 = 15.4
ΔG°0 = 15.2
CS
ΔH°0 = 4.3
ΔG°0 = 4.7

Figure S4

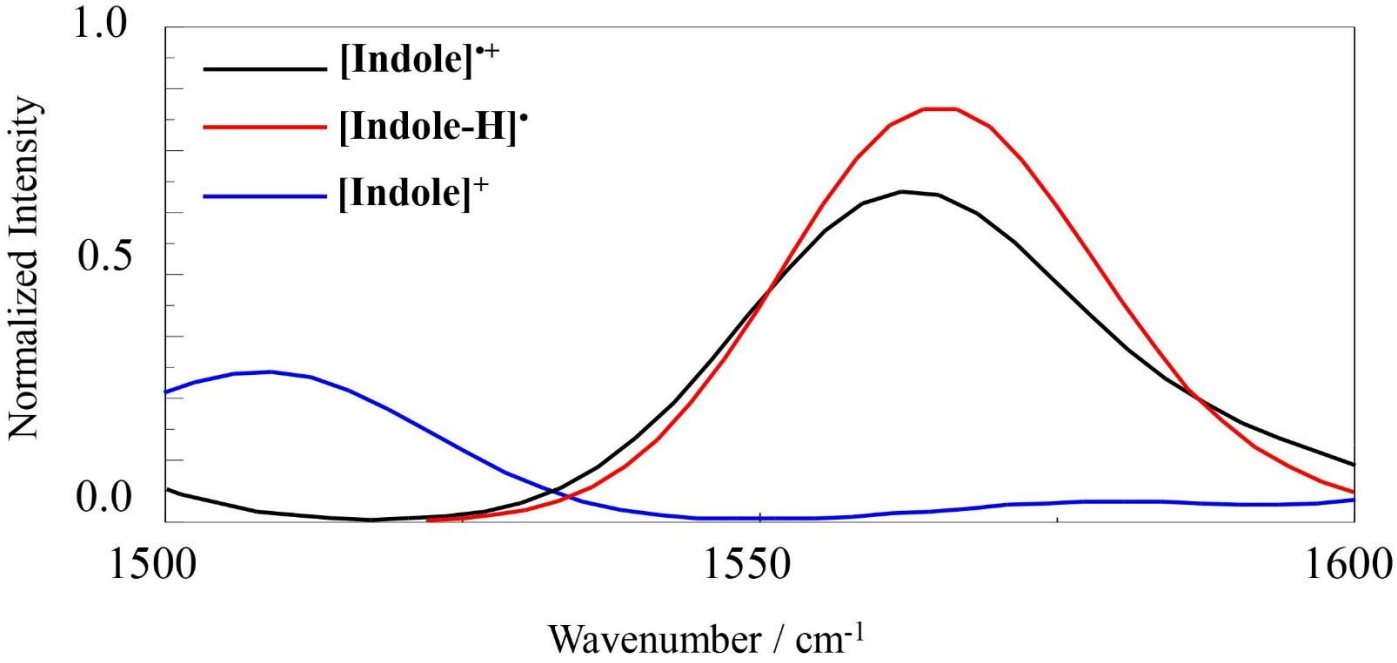
1.0
0.5
0.0
Normalized Intensity
[Indole]•+
[Indole-H]•
[Indole]+
1500
1550
1600
Wavenumber / cm-1

Figure S5

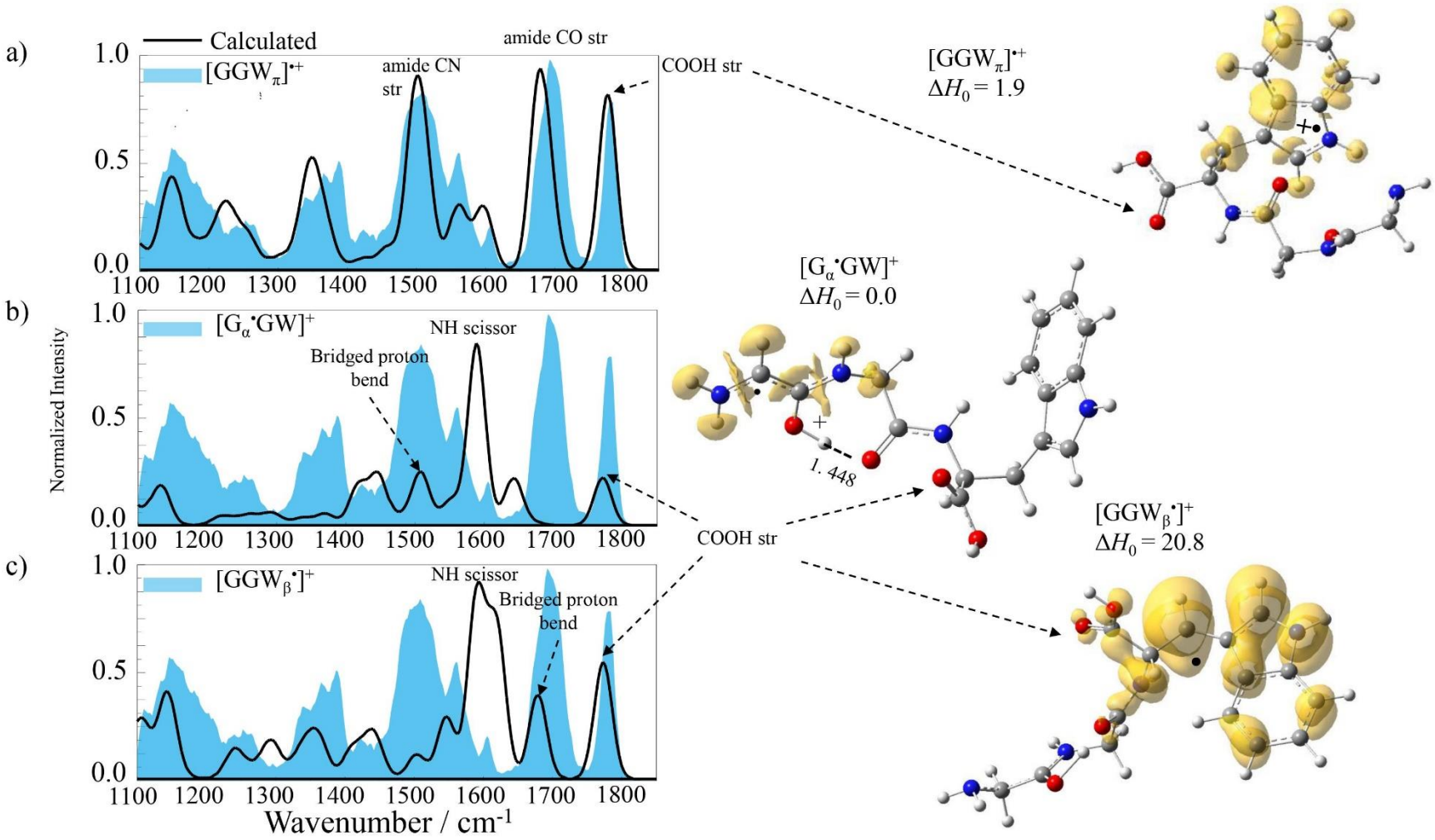
a)
b)
c)
Calculated
[GGW$_\pi$]$^{\bullet+}$
[G$_\alpha$•GW]$^+$
[GGW$_\beta$•]$^+$
amide CO str
amide CN str
COOH str
NH scissor
Bridged proton bend
Normalized Intensity
Wavenumber / cm^{-1}
1.0
0.5
0.0
1100 1200 1300 1400 1500 1600 1700 1800
[GGW$_\pi$]$^{\bullet+}$
ΔH_0 = 1.9
[G$_\alpha$•GW]$^+$
ΔH_0 = 0.0
1. 448
[GGW$_\beta$•]$^+$
ΔH_0 = 20.8

Figure S6

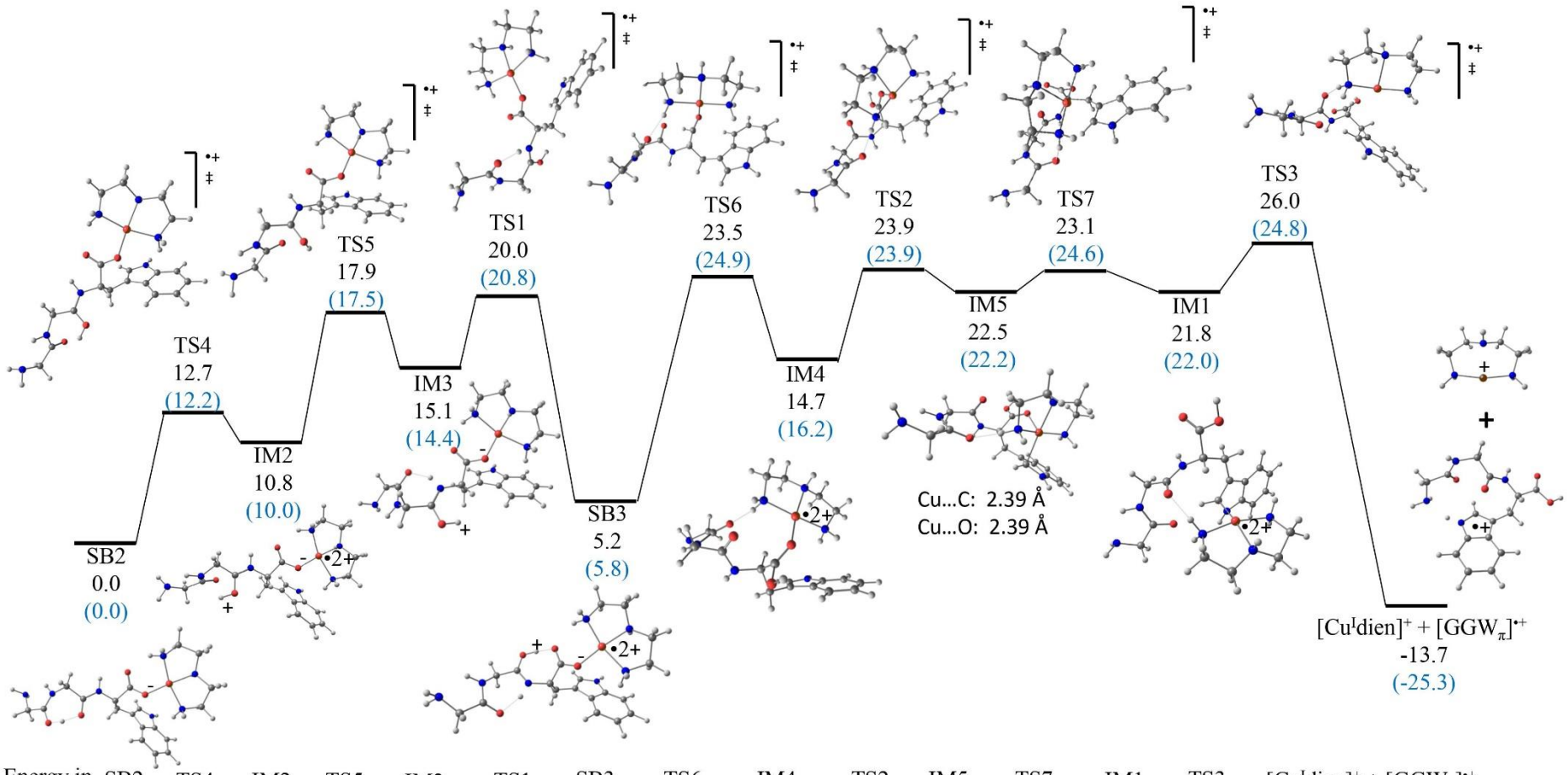
SB2
0.0
(0.0)
TS4
12.7
(12.2)
IM2
10.8
(10.0)
TS5
17.9
(17.5)
IM3
15.1
(14.4)
TS1
20.0
(20.8)
SB3
5.2
(5.8)
TS6
23.5
(24.9)
IM4
14.7
(16.2)
TS2
23.9
(23.9)
IM5
22.5
(22.2)
Cu...C: 2.39 Å
Cu...O: 2.39 Å
TS7
23.1
(24.6)
IM1
21.8
(22.0)
TS3
26.0
(24.8)
[CuIdien]+ + [GGWπ]•+
-13.7
(-25.3)
Energy in kJ mo-1
SB2 0.0 (0.0)
TS4 54.1 (51.2)
IM2 46.3 (42.1)
TS5 76.0 (73.5)
IM3 64.4 (60.2)
TS1 84.6 (87.1)
SB3 23.0 (24.4)
TS6 98.2 (104.1)
IM4 61.5 (67.7)
TS2 99.9 (99.9)
IM5 94.0 (94.0)
TS7 96.6 (102.8)
IM1 91.1 (92.0)
TS3 108.7 (103.7)
[CuIdien]+ + [GGWπ]•+ -57.3 (-105.8)